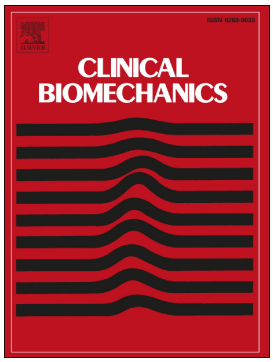

Detection of bridging veins rupture and subdural haematoma onset using a finite element head model

G.F.J. Migueis, F.A.O. Fernandes, M. Ptak, M. Ratajczak, R.J. Alves de Sousa

PII: S0268-0033(18)30661-2
DOI: https://doi.org/10.1016/j.clinbiomech.2019.02.010
Reference: JCLB 4696

To appear in: *Clinical Biomechanics*

Received date: 6 August 2018
Revised date: 13 February 2019
Accepted date: 14 February 2019

Please cite this article as: G.F.J. Migueis, F.A.O. Fernandes, M. Ptak, et al., Detection of bridging veins rupture and subdural haematoma onset using a finite element head model, Clinical Biomechanics, https://doi.org/10.1016/j.clinbiomech.2019.02.010

Detection of bridging veins rupture and subdural haematoma onset using a finite element head model

G.F.J. Migueis[a], F.A.O. Fernandes[a], M. Ptak[b], M. Ratajczak[c], R.J. Alves de Sousa[a,*]

[a] *TEMA: Center of Mechanical Technology and Automation, Department of Mechanical Engeineering, University of Aveiro, Portugal*

[b] *Wroclaw University of Science and Technology Faculty of Mechanical Engineering, Lukasiewicza 7/9, 50-371 Wroclaw, Poland*

[c] *University of Zielona Gora, Faculty of Mechanical Engineering, Prof. Z. Szafrana 4,65-516 Zielona Gora, Poland*

Abstract

Background:

One of the most severe traumatic brain injuries, the subdural haematoma, is related to damage and rupture of the bridging veins, generating an abnormal collection of blood between the dura mater and arachnoid mater. Current numerical models of these vessels rely on very simple geometries and material laws, limiting its accuracy and bio-fidelity.

Methods:

In this work, departing from an existing human head numerical model, a realistic geometry for the bridging veins was developed, devoting special attention to the finite elements type employed. A novel and adequate constitutive model including damage behaviour was also successfully implemented.

Findings:

Results attest that vessel tearing onset was correctly captured, after comparison against experiments on cadavers.

Interpretation

Doing so, the model allow to precisely predict the individual influence of kinematic parameters such as the pulse duration, linear and rotational accelerations in promoting vessel tearing.

Abstract word count: 159 words

Manuscript word count: 3990 words

Keywords: Biomechanics, finite elements, bridging veins, subdural haematoma, head model, damage modelling

*Corresponding author

Email address: rsousa@ua.pt, Campus Santiago, University of Aveiro, 3810-193 Aveiro, Portugal, phone: +351234370200 (R.J. Alves de Sousa)

1. Introduction

The human head is one of the most important parts of the human body since it includes the brain, a vital organ to the human life. Given its importance, head injuries can be quite serious, leading to long-term incapacity or even to death. In road traffic, sports or other accident scenarios, one of the most common types of cerebral injury is the subdural haematoma (SDH), which is also linked to long term incapacity, [Gennarelli (1983)]. Statistically, a third of SDH cases are related with the rupture of the bridging veins (BVs), caused by excessive loading [Besenski (2006); Ho (2008); Kleiven (2002)]. According to Richter et al. (2001), in a total of 409 cases of head injuries, more than half were cerebral injuries, mainly SDH. They can be caused by several types of contact loads, as long as they lead to relative motion between brain and skull, bruising the brain's surface and rupturing the BVs. Following the tangential forces generated between skull and brain, Sahuquillo-Barris et al. (1988), SDH is caused by an excessive short-term tensile-load [Sahuquillo-Barris et al. (1988)] and longitudinal stresses at the veins, ultimately leading to their rupture Asiminei et al. (2011).

The bridging veins are blood vessels which function is to drain the blood from the cerebral cortex to the Superior Sagital Sinus (SSS) [Vignes et al. (2007)], crossing the subdural space. Despite its importance in head impact biomechanics, there is still much to investigate about their histology, morphology and mechanical behaviour, which is fundamental in the creation of reliable finite element models to study their biomechanics.The cranial end of the bridging veins is found at the dura mater and the cerebral end is found on the hemispheres. Unlike the subarachnoid space, where arachnoid trabeculaes exist, the subdural space does not provide any structural support to the bridging veins. While the lateral movement of the brain is impaired and minimized by the presence of the falx, the dura mater descends vertically in the longitudinal fissure between the cerebral hemispheres, and so the antero-posterior movement of the brain has no protective barrier [Yamashima & Friede (1984)]. Furthermore, any head impact that causes this type of movement can lead to a rupture of the bridging veins and consequently bleeding that accumulates in the virtual subdural space [Lee & Haut (1989)].

Acute cases of subdural haematomas (ASDH) are a particular type of SDH usually caused by hemorrhagic contusions that cross the arachnoid matter following veins rupture.Gennarelli & Thibault (1982) reports a incidence of ASDH of 30% with a mortality rate of 60%.

The bridging veins connections into the SSS are not uniformly distributed and their properties may have substantial differences according to specific brain areas [Ratajczak (2016)]. Gender, age and clinical history may also have influence. Han et al. (2007) divided SSS into four segments from the anterior to the posterior part. The author observed that more bridging veins can be found at the first and fourth segments (extremities), compared to the second and third segments. They also concluded that given the many different orientations of the blood flow in the SSS, whatever the movement of the brain in relation to the skull, there

is always a possibility of rupture leading to the appearance of injuries.

Other studies focusing on the BV dimensions were already published and reported by many researchers. Some of their results are presented in table 1. It is possible to observe that the external vessel diameter may vary between 0.5 and 5.3 mm. The same table presents the value for the SSS external diameter, as provided by Monea et al. (2014).

Table 1: Bridging veins dimensions.

Length [mm]	Diameter D_e [mm]	Wall thickness e [mm]	References
10-20	1-3	Subdural: 0.01-0.6 Sub-arachnoid: 0.05-0.2	Yamashima e Friede (1984)
0-70	0.5-5.3	-	Oka et al. (1985)
6.42 (4)	1.4 (0.63)	0.05 (0.02)	Lee e Haut (1989)
- -	0.5-4 1.4-3.1	- -	Sampei et al. (1996)
-	1.84 (0.35)	0.12 (0.02)	Monson (2005)
Male: 22.11 (7.6) Female: 17.92 (5.93)	Male: 2.7 (0.85) Female: 2.71 (1.06)	Male: 0.03 (0.01) Female: 0.04 (0.02)	Delye et al. (2006)
-	0.5-4	-	Vignes et al. (2007)
- -	Dead bodies: 2.5 (1.1) DSA: 3.4 (0.8)	- -	Han et al. (2007)
-	3.42 (1.18)	0.044 (0.017)	Monea et al. (2014)

Kinematically, a head impact results in head acceleration, during a certain time amplitude (pulse), which leads to the inertial loading of intracranial structures. The acceleration can be divided into translational and rotational counterparts. Generally, translational acceleration results in focal brain injuries and rotational acceleration causes diffuse brain injuries. Pure translational acceleration creates intracranial pressure gradients, whereas pure rotational acceleration causes the skull to rotate relative to the brain, which can lead to rupture of the bridging veins [Bandak (1997a)]. However, real head impacts combine both types of acceleration and therefore both types of injuries may occur. Most part of severe head injuries are due to rotational loads once they originate brain tissues and/or bridging veins rupture.

Given the importance of rotational accelerations in the study of head injuries, many authors have investigated the maximum limits that the human head can withstand. Löwenhielm (1978) pointed angular acceleration of 4500 rad/s^2 together with angular velocity of 70 rad/s as critical values for bridging veins rupture. Also regarding the onset of subdural haematoma, Gennarelli & Thibault (1982) pointed to α=32000 rad/^{2}, t=14 ms as critical kinematic parameters, while Depreitere et al. (2006) stated α=10000 rad/s^2 and t>10 ms .

This work will contribute to the knowledge in this field by developing a geometrically detailed and constitutively accurate numerical model of the system comprising the BVs and SSS, integrating it in an

existing head model, and finally validating it against experimental results. In the end, a competent framework for detecting the onset of subdural haematoma is obtained.

2. Finite element models

The development of sophisticated numerical models of the several head parts using, for example, the finite element method aims to predict the mechanical response of the head during an impact. In fact, to better understand the mechanisms that trigger them or to develop prevention and detection mechanisms, many Finite Element Head Models (FEHMs) have been developed, some of them including the Bridging Veins (BVs). These models have been used as a mean of investigation, perception and prediction of human head response under severe impact conditions, once they allow to obtain predictions about the occurrence of head injuries through computational simulations and calculation of stresses and strains fields, which would be impossible to obtain experimentally or analytically [Fernandes & Alves de Sousa (2015); Fernandes et al. (2018c,a)].

In current works focused on mapping bridging veins biomechanics, simple finite element formulations such as beam, discrete beam, truss and spring are being used, among others, using simplified linear-elastic material models. For this reason, these models do not provide a full insight into the behavior of the bridging veins under complex mechanical loads. Summing up, due to the lack of geometrical detail, proper material modeling or correct connection to other brain parts, such representations are still not fully reliable [Famaey et al. (2014)].

From the many models that have already been developed, only those who have bridging veins modeled will be mentioned in this paper: the WSUHIM, as presented by Zhang et al. (2001a) has eleven pares of bridging veins. The KTH FEHM is constituted by the SSS and eleven pares of bridging veins. Ho & Kleiven (2007) studied the influence of including blood vessels and concluded that they are beneficial for the study of ASDH. The YEt Another Head Model (YEAHM) is a recent FEHM [Fernandes et al. (2018e)]. It comprises the brain, skull and a volume that groups the falx, meninges and the cerebrospinal fluid (CSF). This version of YEAHM was validated through simulations of two different well-known experimental tests with cadavers. The first one, by Nahum et al. (1977), measuring the pressure gradient originated in the model when a projectile contacts the skull and the second one, by Hardy et al. (2007), monitoring the brain motion during a head impact. The YEAHM was developed based on medical images from MRI and CT scans [Fernandes et al. (2018e,b)], presenting as main features the geometric detailing of sulci and gyri cerebral structures. Another distinguishing feature is the way head components interact. In this sense, it is allowed the relative motion between the skull and brain, something usually neglected in other head models.

In this work, and in order to upgrade the YEAHM and enable it for the detection of SDH, bridging veins were geometrically and constitutively modeled, assembled in the FEHM and finally validated against experimental data.

3. Constitutive modeling

Although many authors theoretically report that bridging veins may have a hyperelastic behavior (Famaey et al. (2014)), other experimental studies support the thesis that the bridging veins behave as an elastoplastic material [Monea et al. (2014)]. In this work, veins were modeled according to this assumption. In fact, the stress-strain curves reported resemble elastoplastic response curves that may be divided into three distinct phases: a initial phase where the material has an elastic behavior, an intermediate one where the material deforms plastically and finally a final stage that corresponds to the rupture of the material. Doing so, the elastic behaviour is defined by the Young modulus ($E = 25.72$ MPa) and the Poisson ratio ($\nu = 0.45$), after Monea et al. (2014). Plastic properties were assigned by inputting directly the plastic counterpart of the experimental stress-strain curve into Abaqus *plastic material. The Poisson ratio indicates incompressibility, which is typical of most intracranial soft tissues, but will require specific finite element choices to ensure quality of results.

As referred, Monea et al. (2014) presented several stress-strain curves obtained from different uniaxial tests. From them, one curve corresponds to an elongation velocity of 1358.55 mm/s and a strain rate of 136.85 s^{-1}, compatible with head impact scenarios, and shall be here used for material validation purposes. To this end, uniaxial tensile tests were simulated and compared against the experimental curves. To match the experimental setup, a solid vein with an external diameter of 1.5 mm and length 5mm was modeled, being elongated at a constant velocity of 1358.55 mm/s. Explicit time integration scheme in Abaqus was used. The choice of a solid geometry was considered as a valid approximation once no blood (internal) pressure was modelled, and the main objective was to proper reproduce the uniaxial tensile mechanical response. Also, compared to shell elements, solid elements have the ability to deal with full 3D constitutive laws and provide easier imposition of boundary conditions and contact procedures, allowing for more efficient future improvements. Moreover, they allow a convenient treatment of locking pathologies in this case using 2nd order elements. A refined mesh of second order tetrahedrons (C3D10M, volumetric locking free) was employed to avoid numerical pathologies related to incompressibility material conditions [Fernandes et al. (2018e)].

The numerical results computed for the uniaxial stress and strain at the integration points of the elements were compared against the input material data. This comparison is presented in figure 1 (at left). Measured and simulated curves clearly overlaps until the rupture point. Then, an expectable sudden drop on stress

values is reported experimentally, and simulation loses its physical meaning. Given the similarity of numerical and experimental curves until the rupture point, it is possible to confirm the validation of this material model. The next step is the implementation of the damage model with element deletion in order to correctly capture BVs tearing onset and rupture phenomenon.

3.1. Damage modeling

A ductile damage criterion was chosen given its consistency with the experimental observations carried out in Monea et al. (2014), simplicity and straightforward implementation. In fact, vessel tearing has its onset after considerable deformation values, which would be incompatible with brittle-type behaviour. The ductile damage criterion is a phenomenological model that predicts the occurrence of damage due to the appearance of voids [Dassault Systemes (2017)], and may be employed to model soft tissues [Li (2016)]. The model assumes that the equivalent plastic stress at the beginning of damage is a function of the triaxility of the stress and strain rate: $\bar{\varepsilon}_D^{pl}(\eta, \dot{\bar{\varepsilon}}^{pl})$, where $\eta = \frac{-p}{q}$ defines the stress triaxility, p is the pressure stress, q represents the von Mises equivalent stress and the $\dot{\bar{\varepsilon}}^{pl}$ represents the strain rate. The damage criterion is initiated when the following condition is verified, Prantl et al. (2013),:

$$\omega_D = \int \frac{\partial \bar{\varepsilon}_D^{pl}}{\bar{\varepsilon}_D^{pl}(\eta, \dot{\bar{\varepsilon}}^{pl})} = 1 \tag{1}$$

where the ω_D is the damage evolution variable variable that increases with the plastic deformation. At each increment during the analysis, the incremental increase of the ω_D is described as:

$$\Delta\omega_D = \frac{\Delta\bar{\varepsilon}_D^{pl}}{\bar{\varepsilon}_D^{pl}(\eta, \dot{\bar{\varepsilon}}^{pl})} \geq 0 \tag{2}$$

Once the damage initiation criterion is reached, the effective plastic displacement ($\bar{u}^{pl}$) is defined by equation 3, where L represents the element characteristic length, which is defined as very close to zero, to obtain an instantaneous break once rupture strain is achieved.

$$\dot{\bar{u}}^{pl} = L \cdot \dot{\bar{\varepsilon}}^{pl} \tag{3}$$

3.1.1. Validation

The same procedure as in the first validation was used, but this time coupling the damage model. Thus, the stress-strain curve is expected to match the one obtained in the previous simulation, until the ultimate

stress is reached. Then, due to damage and rupture (element deletion), the stress has to abruptly decrease mimicking the experiments.

For this damage model, it is necessary to define four parameters: the stress triaxility, the strain rate, the ultimate strain and the damage evolution coefficient. The ultimate strain and the strain rate, presented in Table 2, are the same ones used in the previous analysis. The stress triaxility was set to 0.33, the natural value under uniaxial stress.

The last parameter, the damage evolution, is dependent on the material behavior in the simulation since it is linked to the material response to the developed stress and strain. Doing so, to proper identify its correct value, simulations were performed using different damage evolution values. Agreement with experiments was obtained for a value of 0.05, as shown in figure 1 (at right).

Table 2: Values used to define the damage criterion.

Ultimate strain	Stress triaxility	Strain rate (s^{-1})	Damage evolution
0.31875	0.33	135.86	0.05

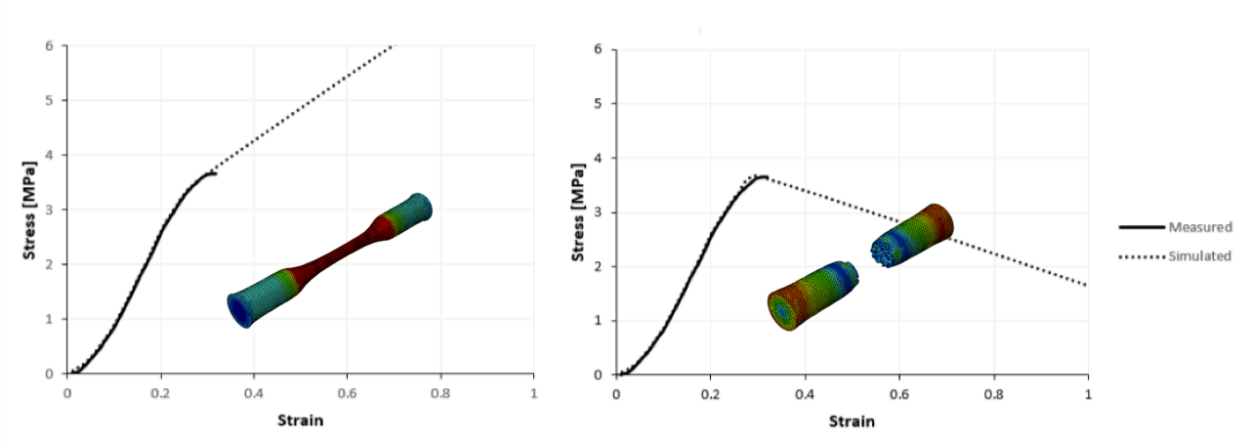

Figure 1: Comparison between experimental curve obtained by Monea et al. (2014) and the numerical one. Left: material modelling not including damage modelling; Right: including damage modelling and element deletion.

A mesh sensitivity study was also carried out. Starting from an average mesh size of 0.1mm, resulting in 7904 nodes, 39742 second order tetrahedral elements, mesh size was progressively increased, keeping material parameters, until the solution started to deteriorate. In this sense, an optimum average mesh size of 0.4mm, 238 nodes and 840 elements was chosen as the optimum choice for mesh parameters. Consequently, they were employed to mesh the BV+SSS geometrical model.

4. Bridging veins geometrical model

After validating the constitutive strategy, the bridging veins geometry was developed. As previously discussed, the choice was to model the SSS+BV set as it ensures greater reliability regarding the kinematics reproduction, and consequently higher precision detecting SDH. Additionally, it ensures a closer approximation to the reality, regarding the relative motion between skull, BV+SSS set and brain. To this end, tie-type connections were made between the brain and the small extensions of the bridging veins, and also between

the SSS and the skull. The vein's length crossing the subdural space is not restrained in any form, although surface-to-surface contact conditions were imposed between BVs and brain. With such boundary conditions, it is guaranteed the correct reproduction of the relative motions between skull and brain, and consequently, vessel stretching upon impact loads. Figure 2 (at left) presents the geometry developed for the SSS+BV set and figure 2 (at right) shows the numbering of the nine BV pairs.

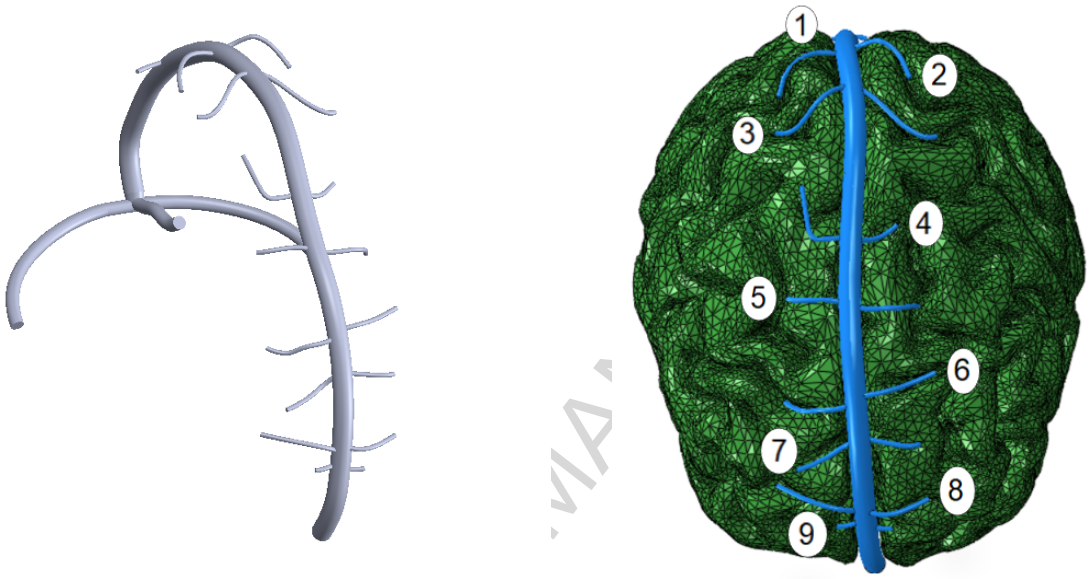

Figure 2: Left: CAD illustration of the SSS+BV set; Right: Bridging veins pairs numbering

According to [Kiliç & Akakin (2008)], there are between eight and twelve pairs of bridging veins in the human head. In this work, nine pairs of veins were geometrically modelled based on medical images (angiograms kindly provided by Hospital Sao Joao, Porto, Portugal, undisclosed) and on anatomical atlas [Nowinski (2016)]. As in the previous validation, the BVs were modeled approximately with 1.5 mm of constant diameter, a value within the range reported in the literature. The diameter of the SSS is 5 mm, once more based on Monea et al. (2014).

4.1. Validation of BVs coupled with YEAHM

Nahum et al. (1977) test was firstly used to understand if the implementation of the bridging veins in the YEAHM had any influence on its overall behavior, since the first version of this finite element head model (without BVs) has already been validated in Fernandes et al. (2018e,d). The test basically consists on impacting a 5.59 kg mass projectile at 9.94 m/s into the forehead area, Figure 3. Although reported in 1977, it is one of the few cadaver tests available, and still widely used for the FEHMs validation. Thus, intracranial pressure was recorded during the impact for different head areas, Figure 4.

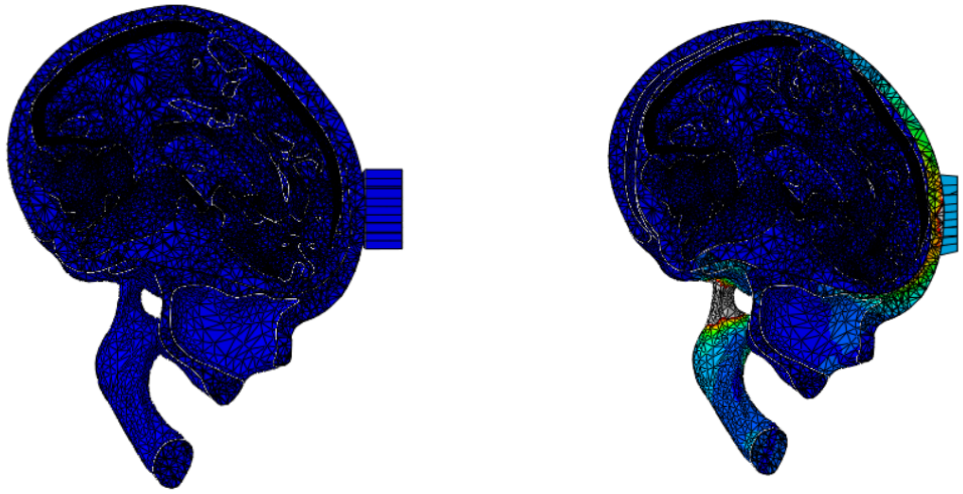

Figure 3: Left:Representation of the simulation beginning for the Nahum et al. (1977) test; right: Cut-out illustration taken during the forehead impact.

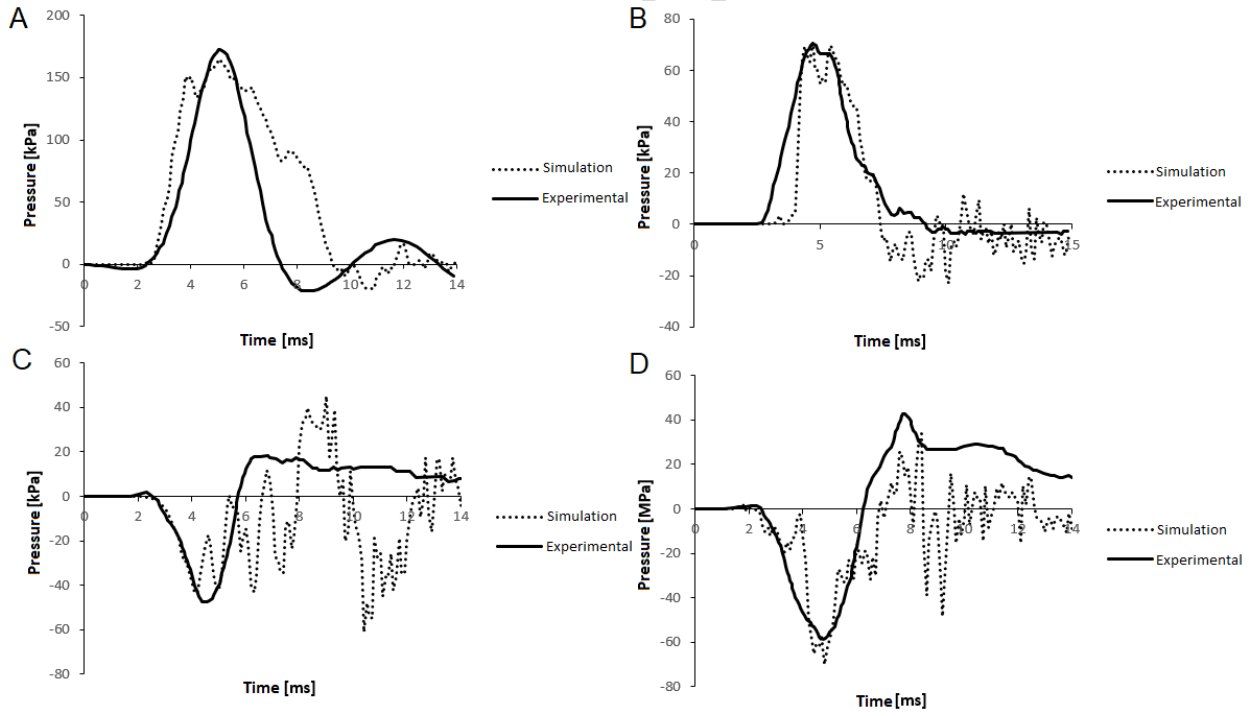

Figure 4: Comparison between intracranial pressures obtained experimentally by Nahum et al. (1977) and the pressures obtained in the simulation. A) - Frontal zone; B) - Parietal zone; C) - Occipital zone and D)- Posterior fossa.

Nahum et al. (1977) observed a high positive pressure peak just below the impact zone in the frontal

area of the head. The pressure levels are lower for the other areas of the head and a negative pressure peak was observed for the posterior part of the head. The same pattern was observed in the simulation performed with this YEAHM version. The simulated curves showed a very good fit compared to the experimental data, and so they were considered close enough to affirm that the YEAHM model with BVs inclusion behaves as well as its original version without BVs. It is worth noting that no occurrence of subdural haematomas could be detected in this present scenario, once the rupture strain was never achieved at BV pairs. Doing so, another test - surely leading to BVs rupture - was carried out.

The test proposed by Depreitere et al. (2006) can be in fact used to validate the model ability to predict vessels tearing and rupture. It will also allow evaluating the influence of kinematic parameters such as pulse duration, as well as the two acceleration components (rotational and translational). The original test in cadavers consisted in launching a pendulum against the back of the head at different impact energies. Using luminescent fluid injected into the veins, it was possible to infer about vessel rupture after a given impact. Since the rotational and linear acceleration time history curves were measured and reported, it is straightforward to recreate these tests. In other words, there is no need to model the pendulum, being sufficient to induce the acceleration time history at the FEHM center of mass.

To perform a parametric study, specific values were chosen from the original tests for inducing the linear and rotational accelerations (Table 3). The objective was to study the individual influence of each kinematic parameter in the rupture onset. Pulse duration was initially fixed to 3.5ms. Then, one acceleration peak value was varied fixing the remaining, simultaneously evaluating the occurrence of tearing in the BV pairs.

Each simulation reference was obtained combining a number (rotational acceleration component) and letter (translational components) characterizing the acceleration peaks in question (Table 3). The results were condensed in figure 5. It is possible to define a clear boundary between critical and non-critical combinations of acceleration components .

Table 3: Acceleration peak values used in this study.

Denomination	Translational [m/s^2]	Denomination	Rotational [rad/s^2]
a	834	1	384
b	2000	2	2500
c	1250	3	5500
-	-	4	10000

Simulation	Acceleration peak	Result
1-a	a=834 m/s^2 / α=384 rad/s^2	No rupture
2-a	a=834 m/s^2 / α=2500 rad/s^2	No rupture
3-a	a=834 m/s^2 / α=5500 rad/s^2	No rupture
4-a	a=834 m/s^2 / α=10000 rad/s^2	Rupture
1-b	a=2000 m/s^2 / α=384 rad/s^2	Rupture
2-b	a=2000 m/s^2 / α=2500 rad/s^2	Rupture
1-c	a=1250 m/s^2 / α=384 rad/s^2	Rupture

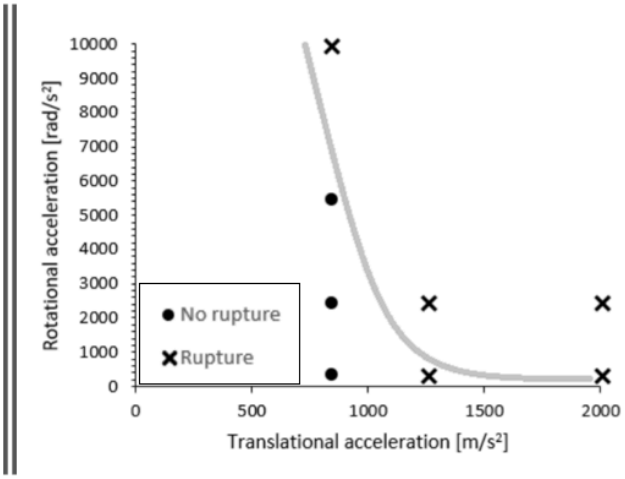

Figure 5: Representation of the obtained results for the different combinations of rotational and translational acceleration components under a fixed pulse.

In this sense, for a fixed pulse value of 3.5 ms, if the linear acceleration is below 1000 m/s^2), a value of 10000 rad/s^2 is necessary to cause rupture on the bridging veins. This value is in accordance with the limit values reported by Depreitere et al. (2006), and slightly higher than the 5000 rad/s^2 reported by Löwenhielm (1978).However, when the linear acceleration increases, specially after 1250 m/s^2, rupture occurs independently of its combined rotational acceleration. To confirm this theory, a final test was performed with an intermediate value of linear acceleration (c=1250 m/s^2), leading to rupture even for a low value of rotational acceleration (384 rad/s^2).

An illustration of the simulated rupture mechanism is given on Figure 6 , where the damage evolution vs. time, of selected BV pairs number 8, is shown (left and right counterparts), regarding test 1b (2000 m/s^2; 384 rad/s^2) until the onset of tearing and final rupture.

In the end, it can be concluded that the influence of linear acceleration is much more decisive than the rotational one. These observations are in agreement with Bandak (1997a), since it was verified that the

linear acceleration enhances the occurrence of focal brain injuries, such as SDH.

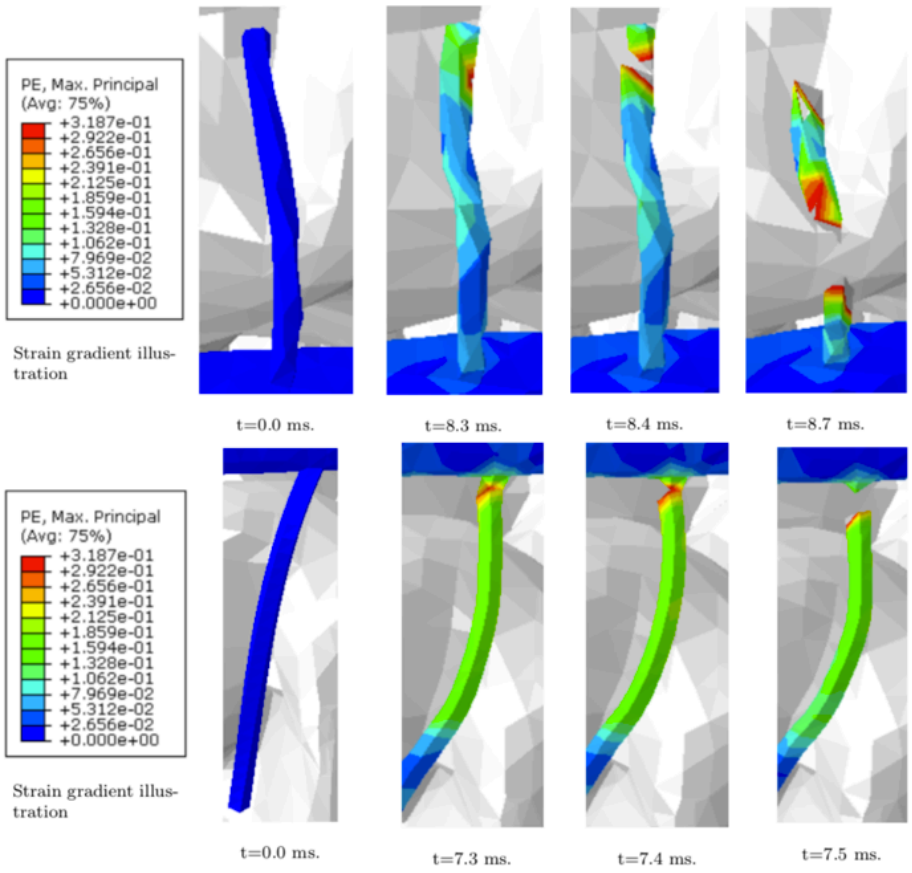

Figure 6: Up:Representation of bridging vein rupture evolution from pair number 8 (left side) for 1-b simulation ((2000 m/s^2; 384 rad/s^2); Down: Representation of bridging vein rupture evolution from pair number 8 (right side) for the same simulation.

4.1.1. Pulse duration

Still under the Depreitere et al. (2006) test conditions, and after studying the influence of linear and rotational acceleration peaks in BVs rupture (pulse duration fixed to 3.5 ms), the influence of the pulse duration was also studied. To this end, new impact durations were set and simulations were done while keeping previous acceleration peaks (v.d. Table 3. Figure 7 summarizes the data of such tests and results in what concerns BV rupture.

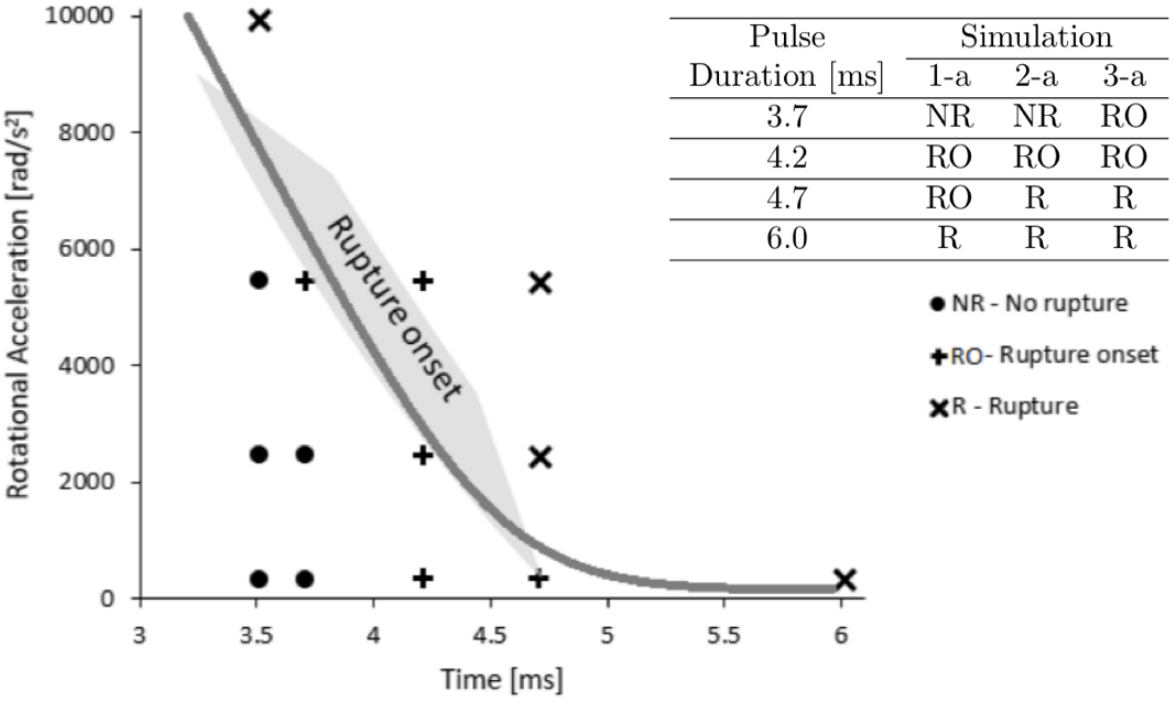

Pulse Duration [ms]	Simulation 1-a	2-a	3-a
3.7	NR	NR	RO
4.2	RO	RO	RO
4.7	RO	R	R
6.0	R	R	R

Figure 7: Representation of the pulse duration vs. rotational acceleration peak.

Three possible outcomes for each test are considered. The first one is NR (No Rupture), and it occurs when no finite element reaches the ultimate strain and for that reason, no severe damage leads to vessel tearing. The second one, RO (Rupture Onset, occurs when just some finite elements that are eliminated during the simulation, but not enough to promote full rupture (here so-called tearing onset). The last, Rupture (R) of the veins, occurs when one or more veins split completely into 2 or more bodies.

Analyzing this new set of results, it is observed that as the rotational acceleration increases, the pulse duration necessary to partially or completely rupture a vein is lower. In fact, it is perfectly acceptable that if acceleration peaks increases (any of its components), a shorter pulse duration is necessary to obtain BVs rupture. The BVs model coupled with YEAHM not only show this standard outcome, but agrees with other thresholds reported in literature.

5. Conclusions and Remarks

The present work can be considered as a first set of developments to better characterize the group of cerebral bridging veins in order to accurately detect the onset of subdural haematoma. The potential of an accurate numerical model than can predict SDH cases is enourmous: from sports to forensics.

Bearing in mind the elaborated anatomical structure involved and complex material properties - often oversimplified in the literature, with many models considering BVs as simple 2 node beam elements - it was particularly important to use a reasonably 3D detailed geometry, proper constitutive equations and advanced finite element technology, dealing with locking pathologies, in the analysis. Particular attention was paid to keep simultaneously CPU efficiency and accuracy.

The uniaxial tests performed showed a perfect agreement regarding the experimental set of dynamic tensile tests performed by Monea et al. (2014), including the accurate prediction of rupture onset. Furthermore, the integration of the set of BVs+SSS into a finite element head model proved capable to predict vessel tearing under complex impact conditions, being validated by directly comparing the results against cadaver experiments. It was possible to attest and confirm the individual influence of kinematic parameters such as the pulse duration, rotational and linear acceleration components. Results also showed that the limit values of strain occurred preferentially in the junction of the bringing veins with the superior sagital sinus. These conclusions are confirmed by clinical studies that describe that most lesions are located within the outflow cuff segment. Nevertheless, the present study did not take into account the variable vein geometry near the cuff segment, and so the rupture site was in fact determined by a stress concentration factor resultant from geometric and boundary conditions.

For a future more detailed analysis, models will need to take into account the directionality of the fibres passing through the vessel, internal pressure, histology and morphology. These studies can be conducted using for instance a multi-scale approach. It should be emphasized that the literature still lacks detailed data from experimental studies, which are the basis for the construction of complex biomechanical models of the cerebral venous system.

In the end, the proposed model proved reliable and capable to be extended to other accident scenarios, such as sports and road traffic injuries.

5.1. Acknowledgement

Center of Mechanical Technology and Automation (TEMA, University of Aveiro) is supported by grants UID/EMS/00481/2013-FCT and CENTRO-01-0145-FEDER-022083. Medical images provided by Hospital Sao Joao (Porto, Portugal) are gratefully acknowledged. Fabio Fernandes is supported by individual grant CEECIND/01192/2017, Fundao para a Cincia e Tecnologia (FCT)

References

Asiminei, A., Baeck, K., Verbeken, E., Sloten, J., & Goffin, J. (2011). Investigation on strain rate dependency in the biomechanical behaviour of the superior sagittal sinus - bridging vein complex. *Proceedings of IRCOBI Conference, Warsaw*, (pp. 36–39).

Bandak, F. (1997a). Biomechanics of impact traumatic brain injury. *Crashworthiness of Transportation Systems: Structural Impact and Occupant Protection*, (pp. 53–93).

Besenski, N. (2006). Imaging of head injuries. *Emergency Radiology: Imaging and Intervention*, (pp. 99–124).

Dassault Systemes, R. U., Providence (2017). Abaqus analysis user's manual, .

Depreitere, B., Van Lierde, C., Sloten, J., Van Audekercke, R., Van der Perre, G., Plets, C., & Goffin, J. (2006). Mechanics of acute subdural hematomas resulting from bridging vein rupture. *J Neurosurg*, *104*, 950–956.

Famaey, N., Ying Cui, Z., Umuhire Musigazi, G., Ivens, J., Depreitere, B., Verbeken, E., & Vander Sloten, J. (2014). Structural and mechanical characterisation of bridging veins: A review. *Journal of the mechanical behavior of biomedical materials.*, *41*, 222–240.

Fernandes, F., & Alves de Sousa, R. (2015). Head injury predictors in sports trauma - a state-of-the-art review. *Journal of Engineering in Medicine*, *229(8)*, 592–608.

Fernandes, F., Alves de Sousa, R., & Ptak, M. (2018a). Application of numerical methods for accident reconstruction and forensic analysis. *SpringerBriefs in Applied Sciences and Technology*, *(9783319899251)*, 59–98. doi:10.1007/978-3-319-89926-8_4.

Fernandes, F., Alves de Sousa, R., & Ptak, M. (2018b). Development of a new finite element human head model. *SpringerBriefs in Applied Sciences and Technology*, *(9783319899251)*, 25–39. doi:10.1007/978-3-319-89926-8_2.

Fernandes, F., Alves de Sousa, R., & Ptak, M. (2018c). Finite element head modelling and head injury predictors. *SpringerBriefs in Applied Sciences and Technology*, *(9783319899251)*, 1–23. doi:10.1007/978-3-319-89926-8_1.

Fernandes, F., Alves de Sousa, R., & Ptak, M. (2018d). Validation of yeahm. *SpringerBriefs in Applied Sciences and Technology*, *(9783319899251)*, 41–58. doi:10.1007/978-3-319-89926-8_3.

Fernandes, F., Tchepel, D., Alves de Sousa, R., & Ptak, M. (2018e). Development and validation of a new finite element human head model - yet another head model (yeahm). *Eng. Comput.*, *35(1)*, 477–496. doi:10.1108/EC-09-2016-0321.

Gennarelli, T. (1983). Head injury in man and experimental animals: Clinical aspects. *Acta Neurochirurgica Supplementum*, *32*, 1–13.

Gennarelli, T., & Thibault, L. (1982). Biomechanics of acute subdural hematoma. *Journal of Trauma*, *22*, 680–686.

Han, H., Tao, W., & Zhang, M. (2007). The dural entrance of cerebral bridging veins into the superior sagittal sinus: an anatomical comparison between cadavers and digital subtraction angiography. *Neuroradiology*, *49 (2)*, 169–175.

Hardy, W., Mason, M., Foster, C., Shah, C., Kopacz, J., Yang, K., King, A., Bishop, J., Bey, M., Anderst, W., & Tashman, S. (2007). A study of the response of the human cadaver head to impact. *Stapp Car Crash Journal.*, *51*, 17–80.

Ho, J. (2008). Generation of patient specific finite element head models. *Doctoral Thesis, Division of Neuronic Engineering, School of Technology and Health, Royal Institute of Technology, Trita-STH Report*, .

Ho, J., & Kleiven, S. (2007). Dynamic response of the brain with vasculature: A three-dimensional computational study. *Journal of Biomechanics*, *40*, 3006–3012.

Kiliç, T., & Akakin, A. (2008). Anatomy of cerebral veins and sinuses. *Front. Neurol. Neurosci.*, *23*, 4–15.

Kleiven, S. (2002). Finite element modeling of the human head. *Doctoral Thesis, Technical Report,School of Technology an Health, Royal Institute of Technology, Stockholm, Sweden.*, .

Lee, M., & Haut, R. (1989). Insensitivity of tensile failure properties of human bridging veins to strain rate: Implications in biomechanics of subdural hematoma, . *22*, 537–542.

Li, W. (2016). Damage models for soft tissues: A survey. *Journal of Medical and Biological Engineering*, *36*, 285–307.

Löwenhielm, P. (1978). Tolerance levels for bridging vein disruption calculated with a mathematical model. *Journal of Bioscience and Bioengineering*, *2*, 501–507.

Monea, A., Baeck, K., Verbeken, E., Verpoest, I., Sloten, J., Goffin, J., & Depreitere, B. (2014). The biomechanical behaviour of the bridging vein-superior sagittal sinus complex with implications for the mechanopathology of acute subdural haematoma. *J. Mech. Behav. Biomed. Mater.*, (pp. 155–165).

Nahum, A., Smith, R., & Ward, C. (1977). Intracranial pressure dynamics during head impact. *Proceeding of 21st Stapp Car Crash Conference*, (pp. 339–366).

Nowinski, W. (2016). The human brain, head and neck in 2953 pieces. *Thieme Medical Publishers*, .

Prantl, A., J.Ruzicka, Spaniel, M., Moravec, M., Dzugan, J., & Konopk., P. (2013). Identification of ductile damage parameters. *2013 SIMULIA Community Conference, Vienna, Austria*, .

Ratajczak, S. M. B. R., M. (2016). An analysis of the effect of impact loading on the destruction of vascular structures in the brain. *Acta of Bioengineering and Biomechanics*, *18*, 21–31.

Richter, M., Otte, D., Lehmann, U., Chinn, B., Schuller, E., Doyle, D., Sturrock, K., & Krettek, C. (2001). Head injury mechanisms in helmet-protected motorcyclists: Prospective multicenter study. *Journal of Trauma*, *51*, 949–958.

Sahuquillo-Barris, J., Lamarca-Ciuro, J., Vilalta-Castan, J., Rubio-Garcia, E., & Rodriguez-Pazos, M. (1988). Acute subdural hematoma and diffuse axonal injury after severe head trauma. *Journal of Neurosurgery*, *68(6)*, 894–900.

Vignes, J., Dagain, A., Guerin, J., & Liguoro, D. (2007). A hypothesis of cerebral venous system regulation based on a study of the junction between the cortical bridging veins and the superior sagittal sinus. *Laboratory investigation. J. Neurosurg.*, *107*, 1205–1210.

Yamashima, T., & Friede, R. (1984). Why do bridging veins rupture into the virtual subdural space? *J. Neurol. Neurosurg. Psychiatry*, *47 (2)*, 121–127.

Zhang, L., Yang, K., Dwarampudi, R., Omori, K., Li, T., Chang, K., Hardy, W., Khalil, T., & King, A. (2001a). Recent advances in brain injury research: a new human head model development and validation. *Stapp car crash journal*, *45*, 369–394.

Highlights

- Detailed numerical modeling of the superior sagittal sinus and 9 pairs of bridging veins
- Constitutive modelling including elasto-plasticity and ductile damage
- Integration into a finite element head model and validation against experiments on cadavers

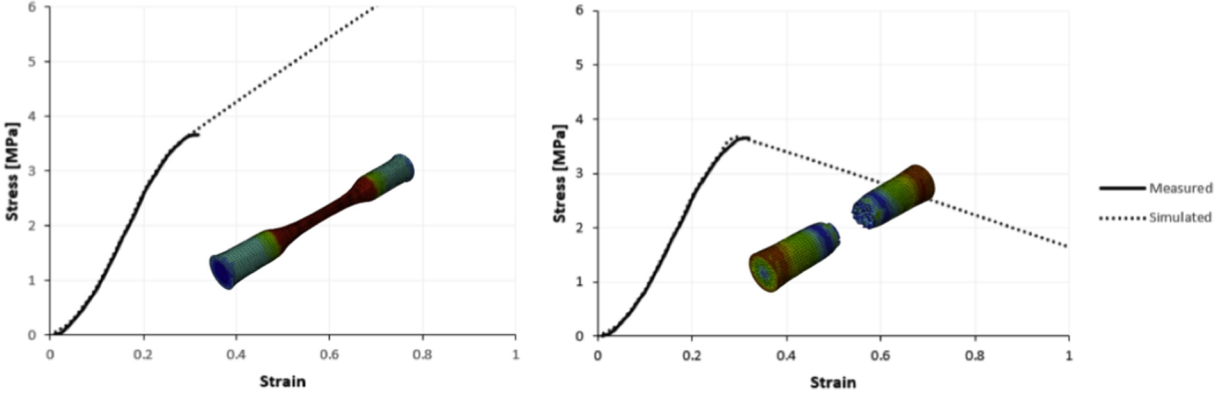

Figure 1

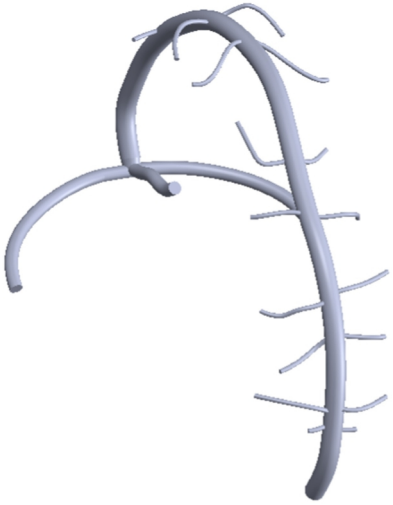

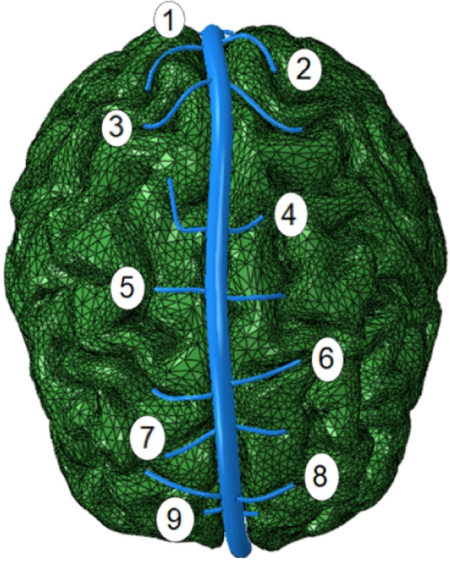

Figure 2

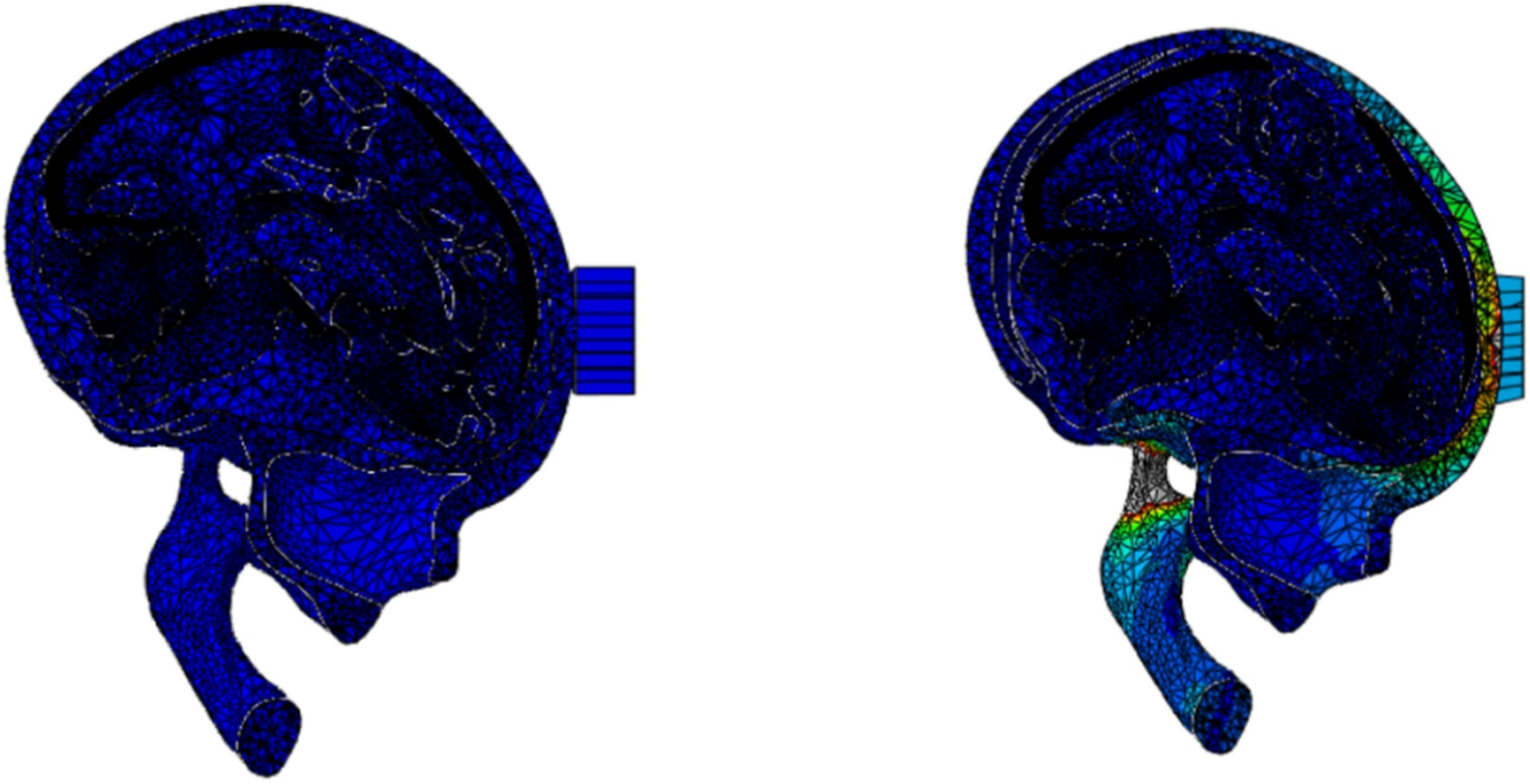

Figure 3

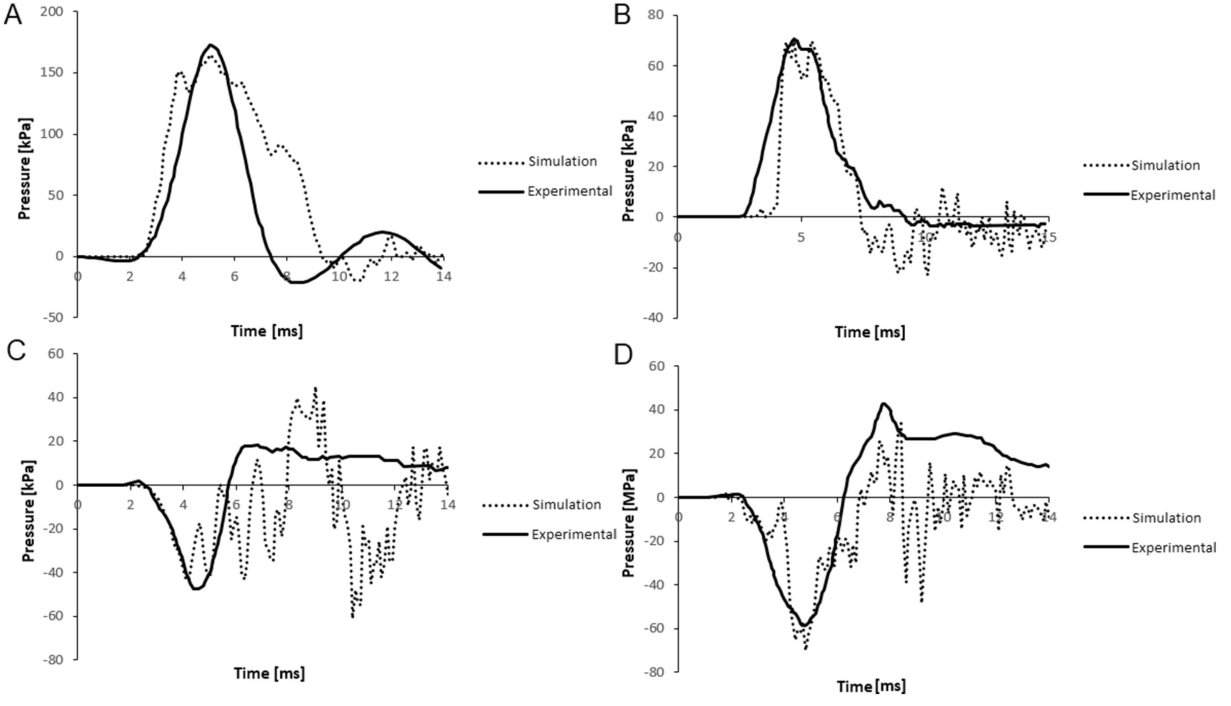
A
Pressure [kPa]
Time [ms]
Simulation
Experimental
B
Pressure [kPa]
Time [ms]
Simulation
Experimental
C
Pressure [kPa]
Time [ms]
Simulation
Experimental
D
Pressure [MPa]
Time [ms]
Simulation
Experimental

Figure 4

Simulation	Acceleration peak	Result
1-a	a=834 m/s^2 / α=384 rad/s^2	No rupture
2-a	a=834 m/s^2 / α=2500 rad/s^2	No rupture
3-a	a=834 m/s^2 / α=5500 rad/s^2	No rupture
4-a	a=834 m/s^2 / α=10000 rad/s^2	Rupture
1-b	a=2000 m/s^2 / α=384 rad/s^2	Rupture
2-b	a=2000 m/s^2 / α=2500 rad/s^2	Rupture
1-c	a=1250 m/s^2 / α=384 rad/s^2	Rupture

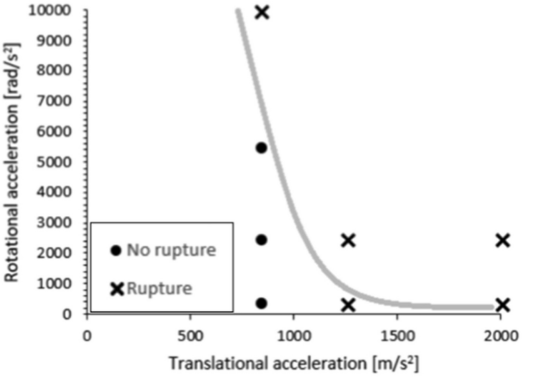

Figure 5

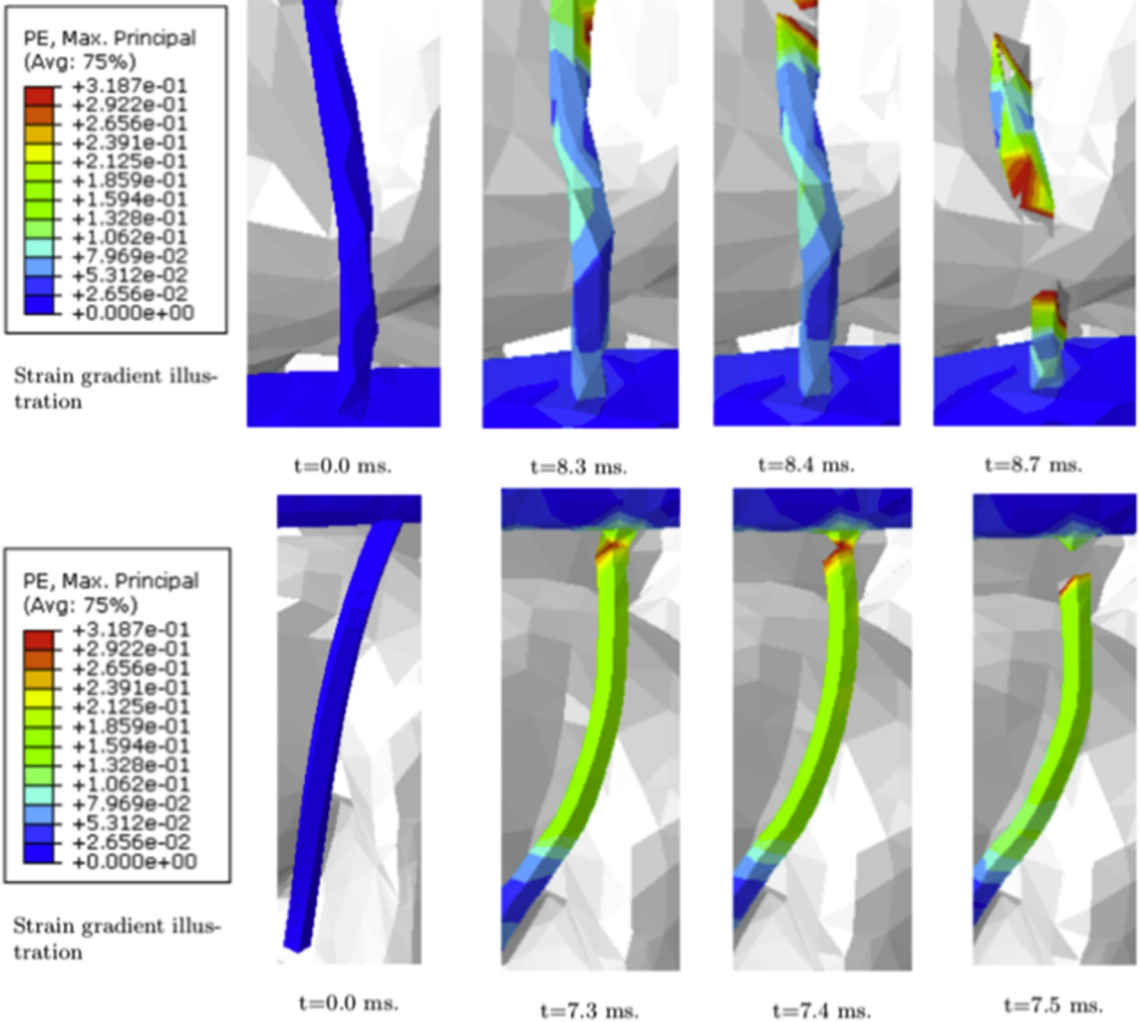
PE, Max. Principal
(Avg: 75%)
+3.187e-01
+2.922e-01
+2.656e-01
+2.391e-01
+2.125e-01
+1.859e-01
+1.594e-01
+1.328e-01
+1.062e-01
+7.969e-02
+5.312e-02
+2.656e-02
+0.000e+00
Strain gradient illustration
t=0.0 ms.
t=8.3 ms.
t=8.4 ms.
t=8.7 ms.
PE, Max. Principal
(Avg: 75%)
+3.187e-01
+2.922e-01
+2.656e-01
+2.391e-01
+2.125e-01
+1.859e-01
+1.594e-01
+1.328e-01
+1.062e-01
+7.969e-02
+5.312e-02
+2.656e-02
+0.000e+00
Strain gradient illustration
t=0.0 ms.
t=7.3 ms.
t=7.4 ms.
t=7.5 ms.

Figure 6

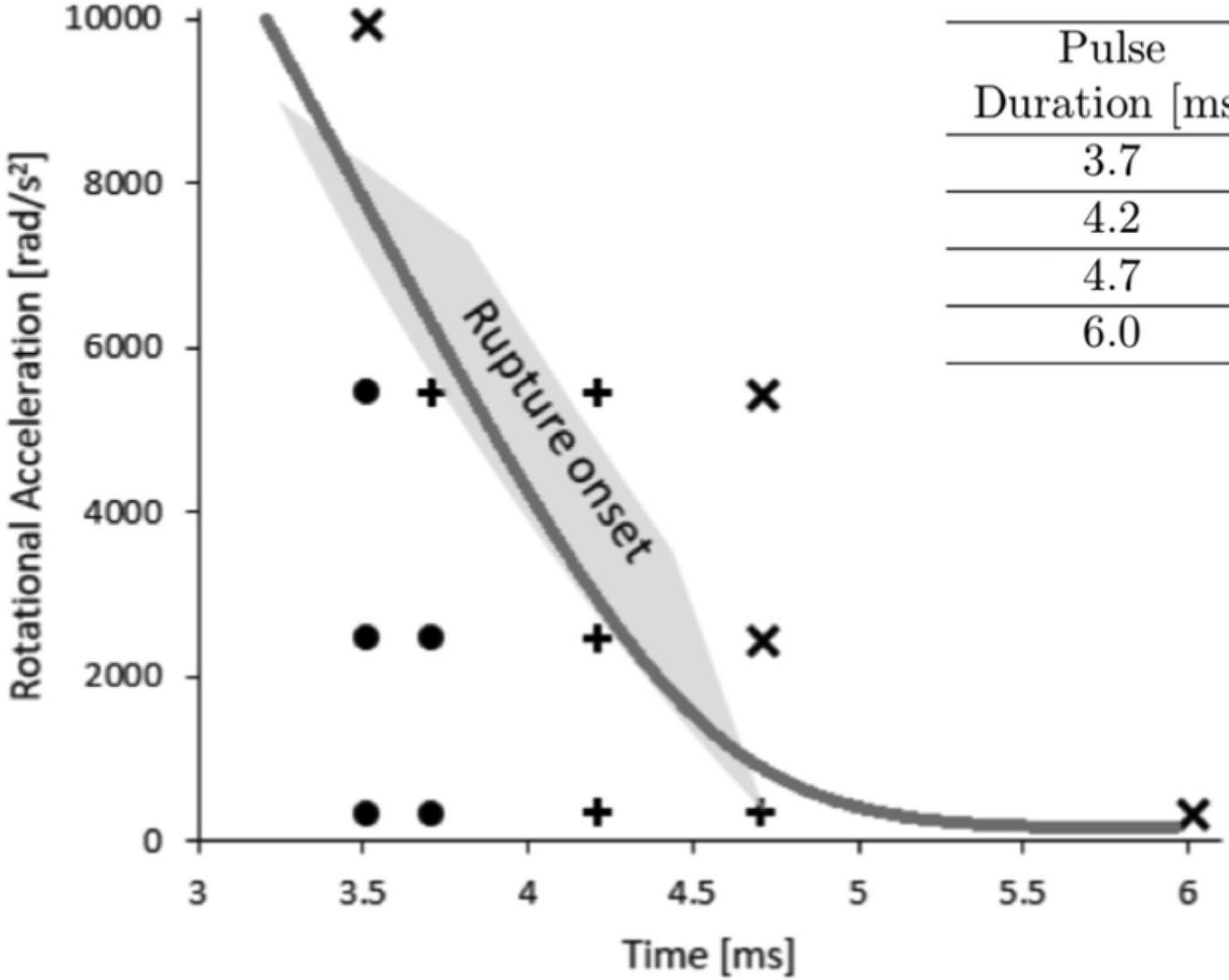

Pulse Duration [ms]	Simulation 1-a	2-a	3-a
3.7	NR	NR	RO
4.2	RO	RO	RO
4.7	RO	R	R
6.0	R	R	R

Figure 7